PROGRESS IN PHOTOVOLTAICS: RESEARCH AND APPLICATIONS
Prog. Photovolt: Res. Appl. (2012)
Published online in Wiley Online Library (wileyonlinelibrary.com). DOI: 10.1002/pip.2229

APPLICATION

Initial field performance of a hybrid CPV-T microconcentrator system

M. Vivar[1]*, V. Everett[1], M. Fuentes[2], A. Blakers[1], A. Tanner[3], P. Le Lievre[3] and M. Greaves[3]

[1] Centre for Sustainable Energy Systems, Australian National University, Canberra 0200, Australia
[2] Grupo IDEA, Universidad de Jaen, Jaen 23071, Spain
[3] Chromasun Inc., San Jose, California, USA

ABSTRACT

The first prototype of the hybrid CPV-T ANU-Chromasun micro-concentrator has been installed at The Australian National University, Canberra, Australia. The results of electrical and thermal performance of the micro-concentrator system, including instantaneous and full-day monitoring, show that the combined efficiency of the system can exceed 70%. Over the span of a day, the average electrical efficiency was 8% and the average thermal efficiency was 50%. Copyright © 2012 John Wiley & Sons, Ltd.

KEYWORDS
concentrator; photovoltaic; thermal; hybrid

***Correspondence**
M. Vivar, Centre for Sustainable Energy Systems, Australian National University, Canberra, 0200, Australia.
E-mail: marta.vivar@anu.edu.au

Received 17 December 2011; Revised 15 March 2012; Accepted 4 April 2012

1. INTRODUCTION

The Australian National University (ANU) has been developing parabolic and linear-focus solar concentrating systems for 15 years. To date, the ANU has installed around 500 m^2 of concentrator trough collectors at two main sites: one in Rockingham, Western Australia, and the other on the roof of Bruce Hall, a residential college on the ANU campus in the ACT. Several smaller, experimental systems are in use at the ANU and at Spring Valley. The first versions of solar concentrator systems developed at the Centre for Sustainable Energy Systems at ANU were purely photovoltaic linear concentrator systems. Later developments included the addition of active cooling to extract the heat, producing a hybrid PV-thermal system.

The Rockingham PV concentrator is a photovoltaic trough concentrator system developed by ANU and Solahart Industries and installed in Rockingham, Western Australia, in 2000 [1]. With a generation capacity of 20kWp, the dual-axis tracking system comprises 80 trough modules with a total aperture area of 150 m^2. Each trough module consists of one parabolic mirror with one solar PV receiver working at a concentration ratio of approximately 25 suns (Figure 1 (a)). The mirrors were constructed using a laminated glass structure with an encapsulated silver film in a parabolic profile, providing an optical reflectivity of 91%. The system used mono-crystalline concentrator silicon cells, with an average efficiency close to 22% at 30 suns and 35 °C, manufactured in Centre for Sustainable Energy Systems laboratories. The cells were bonded to a passive heat sink (aluminium base + aluminium fins) that kept the cells working at a temperature between 30–40 °C above ambient temperature (Figure 1(b)), encapsulated within the receivers with Wacker silicone, and protected by a glass cover. Each receiver has a power rating of 250 Wp. The system was connected to the grid in 2000.

The Bruce Hall Combined Heat and Power Solar system (CHAPS) is a 300-m^2 photovoltaic-thermal hybrid linear concentrator system [2]. This system features a hybrid concentrator receiver that improves overall system efficiency by combining thermal and electrical conversion of solar energy. The solar cells are cooled by a thermal transfer fluid flowing in a channel behind them. The collected thermal energy can be used for hot water storage or heating. The projected annual generating capacity of the CHAPS system installed at ANU is 50 MWh electrical and 360 GJ thermal (domestic hot water). Primary operating results show a total combined (electrical plus thermal) efficiency of the system close to 60%.

The CHAPS system was installed on the roof of the Bruce Hall Packard Wing (Figure 2(a)). This is a four-storey

(a)

(b)

Figure 1. The ANU 20kWp PV trough concentrator at Rockingham (WA, Australia): (a) Aerial view of the complete system and (b) detail of the passively cooled solar concentrator PV receiver.

building providing residential accommodation for 98 students at the ANU. The orientation of the building is rotated 37° to the east away from True North. The PV-thermal hybrid installation incorporates eight roof-mounted single-axis reflective solar concentrating collectors (Figure 2(b)), operating at a concentration level of 38X. Each collector is 24 m long and comprises a tracking support structure controlled by a microprocessor.

The optical system consists of 17 mirror panels made from 1-mm thick rear-silvered glass laminated to a 1-mm

(a)

(b)

Figure 2. The CHAPS PV-thermal hybrid concentrator on the roof of the Bruce Hall Packard Wing: (a) View of the complete system, (b) detail of the PV-T receiver.

thick galvanised steel sheet with stamped tab ribs fitted to each mirror end to ensure the correct profile. The photovoltaic system uses mono-crystalline solar cells, manufactured at ANU, with an efficiency of 20% at 25 °C and 30 suns concentration. The cells are actively cooled, with the heat removed using a thermal transfer fluid flowing through the receiver and passing through a heat exchanger to transfer heat to the hot water storage tanks. There are two banks of central storage tanks, and an additional circuit for the hydronic heating (Figure 3). The system also includes gas boosters for periods when there is insufficient solar power.

The CHAPS PV-thermal concentrator system demonstrates the importance of an over-temperature control. There is the potential to overheat the PV components in the receiver if the thermal supply is not balanced by demand. One solution to this problem is the use of radiators, which are convective units through which the heat transfer fluid is diverted once the receiver reaches 80 °C. The main conclusion drawn from the CHAPS project is

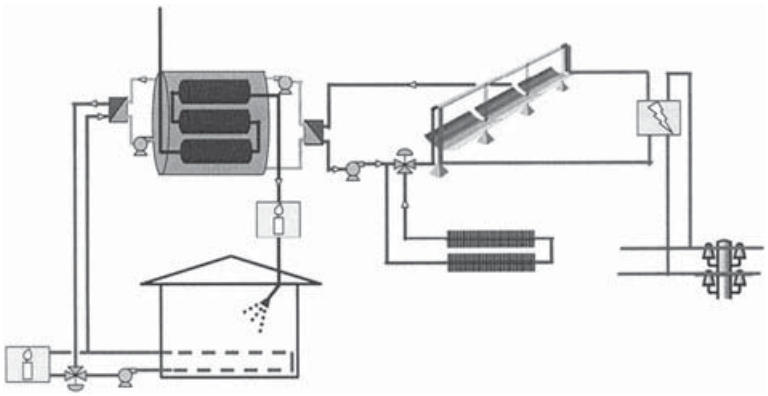

Figure 3. Schematic of the PV-thermal CHAPS hybrid concentrator.

that the cost for conventional PV solar generation using linear concentrators may be reduced by utilising highly efficient solar cells or by using combined PV-thermal hybrid systems to reach higher total efficiencies.

With the experience and knowledge gained from previous PV-T concentrator systems, ANU partnered with the US-based company Chromasun Inc. to jointly develop a hybrid, linear CPV-thermal (CPV-T) micro-concentrator (MCT) system designed specifically for rooftop applications [3]. The Chromasun MCT is a glazed, fully sealed, light-weight structure with a low wind-load factor. The PV-T hybrid version incorporates modified one-sun solar cells operating at around 20X geometric concentration and incorporates a novel, ultra-lightweight Fresnel mirror collector with closed-loop tracking. The MCT produces electricity as well as thermal energy suitable for generating hot water, running absorption chillers, or augmenting heat-pump systems.

A prototype MCT has been installed on the rooftop test area at the Research School of Engineering at ANU (Canberra, Australia) [4]. The first results of the electrical and thermal performance of the ANU–Chromasun hybrid MCT prototype installed at ANU, as well as its main characteristics, benefits and limitations, are presented in this work. These results, including instantaneous and full-day monitoring, show that the combined efficiency of the system can exceed 70%.

2. HYBRID CPV-T MCT DESCRIPTION

The MCT system consists of a fully sealed enclosure that houses two linear Fresnel mirror collectors [5] and two hybrid PV-T receivers [6,7] for the delivery of electricity and hot water for domestic applications (Figure 4, Figure 5 (a)). The MCT enclosure is 3.25 m long, 1.23 m wide and 0.314 m deep, with a total aperture area of 3.5 m^2. The linear Fresnel mirror collector array, comprising two sets of mirrors, each with 10 mirror elements, tracks within the enclosure on a single axis over $\pm 70^\circ$ [8] to focus the sunlight onto its own receiver. The receivers use modified one-sun mono-crystalline silicon solar cells operating at a geometric concentration ratio of 20X, with the cells actively cooled by thermal transfer fluid circulating through an aluminium extrusion at the rear of the receiver.

This recent development has significant advantages over previous developments of hybrid PV-T systems at ANU, including:

- On-site generation of both thermal and electrical energy, with a low-profile system that can be integrated in commercial and domestic buildings;
- Zero exposure to hail, snow, rain, dust and other soiling sources on the mirrors, as they are fully enclosed within the sealed system;
- Elimination of wind loading on the mirror arrays, as they are in a low profile, compact structure and protected within the sealed enclosure;
- Full protection of all the functional components from the external environment, including the receivers, electronics, tracking mechanism, sensors, and mirror arrays, reducing degradation caused by outdoor exposure; and
- Light-weight system, with a total weight loading of approximately 30 kg/m^2, making the MCT suitable for rooftop installation and retro-fitting on almost any structure.

Figure 4. Micro-concentrator system on Santa Clara University Solar Decathlon House, 2010. The three MCT units were mounted on the same PV supports vacated by previously installed PV panels.

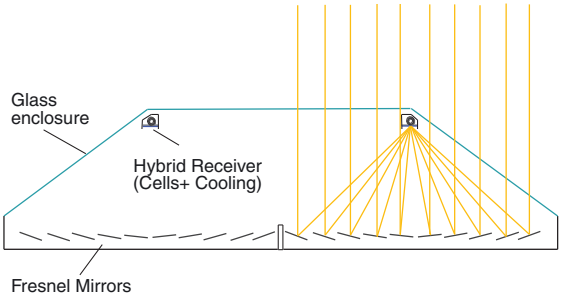

(a)

(b)

(c)

(d)

Figure 5. (a) Schematics of the MCT system showing the glass enclosure and the two sets of Fresnel mirrors with their corresponding hybrid receivers (including the solar cells and the active cooling for the production of heat), (b) an image of one linear Fresnel mirror collector in the MCT under tracking showing the focal features at the receiver surface, (c) conventional one-sun solar cells modified by ANU to function as concentrator cells are soldered to a thermal management substrate, (d) the ANU-Chromasun microconcentrator system installed at ANU (Canberra, Australia).

2.1. Collector: linear Fresnel mirror array

The collector has a linear Fresnel mirror array (Figure 5(b)) constructed from 0.3-mm thick aluminium with a front-mirrored silver surface with a reflectivity of 95% manufactured by Alanod (Alanod MIRO®) [9]. The MCT array comprises two sets of mirrors, with 10 mirrors per set. Each of these mirrors is 3134 mm long by 54 mm wide, providing a total aperture area of 1.75 m^2 per receiver, or 3.5 m^2 per MCT unit. The average focal length is about 256 mm (see Table I). In contrast with conventional concentrator systems, all the mirrors consist of one continuous optical surface, so there are no losses associated with gaps between mirrors in the longitudinal direction.

2.2. Hybrid PV-T receiver

The MCT receivers use one-sun mono-crystalline silicon solar cells that have been modified by ANU to function efficiently as concentrator cells. The cells are soldered to a thermal substrate (Figure 5(c)), and then bonded to a heat sink with a highly thermally conductive adhesive. The cooling fluid circulated through the channel at the rear of the heat sink is used to cool the cells and to extract the heat for domestic hot water applications. Secondary optics are included in the form of small winglets made of reflective silver Alanod placed adjacent to both ends of the cells at the edge of the receiver. The final encapsulation (Figure 6) uses clear silicone Wacker Silgel 612.

The cells are mounted onto sub-modules containing 30 cells each, all electrically connected in series, including four bypass diodes per sub-module. Each PV-T receiver within the MCT enclosure comprises 10 sub-modules electrically connected in series. Finally, the MCT incorporates two receivers, one per set of mirror arrays, which can be electrically connected either in series or in parallel. The two receivers are usually thermally connected in series within the box, although parallel connection is possible. Table II summarises the main characteristics of the receiver design.

One-sun, modified solar cells for concentrators achieved efficiencies between 19 and 19.8% for concentration levels of 20X and 15X, respectively [4]. Once encapsulated into 30-cell sub-modules and connected electrically in series, the sub-modules were characterised at 1 sun and 15 suns illumination. For the 1-sun measurement, indoor Flash I-V equipment was used. For the concentration test, a test rig of smaller size, but replicating all the components of the entire box with the exception of the glass cover, was constructed specifically for test purposes. The average efficiency obtained at 1000 W/m^2 and 25 °C sub-module temperature was approximately 17.3% for the initial batch of 60 sub-modules. Under 15X concentration in the test rig, 950 W/m^2 of DNI and 55 °C fluid temperature circulating on the back of the cells, efficiencies averaged 15%.

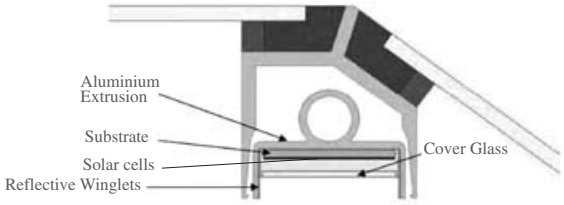

(a)

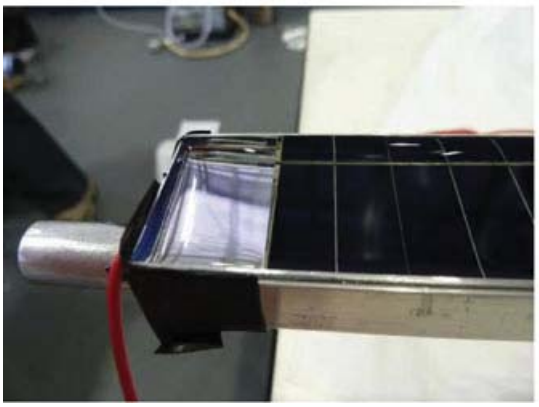

(b)

Figure 6. Hybrid CPV-T receiver: (a) Cross section of the MCT receiver design, featuring the cells soldered to the thermal substrate, the heat sink and fluid channel for active cooling, the glass cover, the reflective winglets as secondary optics and the encapsulation; (b) a functional CPV-T MCT prototype receiver, showing the cells, the encapsulation and the heat sink.

Table I. Main characteristics of the mirror design.

Mirror characteristic	Value
Mirror length [mm]	3134
Number of mirrors per receiver	10
Mirror width [mm]	54
Space between mirrors [mm]	2
Total mirror area width per receiver [mm]	558
Total collector net aperture area per receiver [m^2]	1.75
Total collector net aperture area per box (2 rx's) [m^2]	3.5
Mirror thickness [mm]	0.3
Weight per square metre per box [kg/m^2]	<30
Reflectivity–Alanod Miro Silver [9] [%]	95
Focal length (mm)	256

Table II. The features of the receiver design.

Receiver feature	Value
Cell length [mm]	27.5
Cell width [mm]	9.65
Geometric concentration [suns]	20.3
Number of cells per sub-module	30
Cell interconnections within a sub-module	Series
Number of sub-modules per receiver	10
Sub-module interconnections within a receiver	Series
Number of receivers per MCT unit	2
Receiver interconnections within an MCT unit	Series or parallel

Two full-sized receivers, each comprising 10 series-connected sub-modules, were manufactured and characterised under 1 sun AM1.5G illumination and with the receiver surface normal to the incident sunlight. Measured efficiencies for two prototype receivers were 18.5 and 17.9% at 1000 W/m^2 global irradiance and 15 °C ambient temperature, when measured under direct sunlight outside the MCT unit.

3. SET-UP AND MEASUREMENT PROCEDURE

The first hybrid PV-T MCT prototype has been installed on the rooftop test area at the Research School of Engineering at ANU (Canberra, Australia), as shown in Figure 5(d). Canberra is located 35.3° south and 149.1° east at an altitude of 600 m. The MCT system is oriented on a polar north–south axis, on a structure with adjustable tilt angle that can be varied depending on the season, or for various characterisation tests.

As part of the set-up, a basic cooling circuit for the photovoltaic cells was connected for the initial characterisation tests. Under normal operation, this cooling circuit would provide the hot water for domestic applications in the fully operational system. The cooling circuit consisted of an immersed water pump in a small non-insulated storage tank, with a control valve to regulate the flow rate. The storage tank was filled with ordinary tap water. An alternative arrangement, used for a constant temperature inlet, had the circuit directly connected to the main water supply.

When monitoring the system, two groups of data were recorded: meteorological and system data. Meteorological data included the normal direct irradiance measured using a Kipp and Zonnen Pyrheliometer CH1, the global irradiance on the plane measured by the reference cell from the electronic capacitive load PVPM6020C, and the ambient temperature measured by a K-type thermocouple. A Datataker DT80 data logger was used to monitor all the main parameters.

System data included electrical and thermal data. For the electrical data, the complete *I–V* curve was measured using a PVE PVPM6020C electronic capacitive load. Thermal system data included the inlet and outlet temperatures, measured with waterproof K-type thermocouples, and the flow rate of the cooling liquid, measured with a flow metre.

4. EXPERIMENTAL RESULTS

First results from the electrical and thermal performance of the MCT prototype installed at ANU are presented here, including results from instantaneous and full-day monitoring.

4.1. Instantaneous performance

Instantaneous performance measurements include two possible receiver electrical interconnection configurations within the system: series and parallel, shown in Table III. The cooling circuit was always connected in series within the box, so the temperature change across each receiver is effectively half of the total temperature change. The data obtained from these measurements are representative of general system performance under these test conditions. These data are the results of measurements taken on 25 August 2011 in Canberra, which is in winter; so the elevation tilt angle used for this test was 46 degrees.

Figure 7 shows the instantaneous *I–V* curves of the system prototype for a series receiver interconnection of the two receivers comprising the MCT, and for a parallel receiver interconnection. The results for a measurement at local solar noon are shown in Table IV. At this time, the effective direct irradiance incident onto the MCT system was 997 W/m^2, and both receivers were illuminated evenly. For both receiver-connection configurations, the inlet water temperature was 36 °C and the outlet temperature was 42 °C. Tables V and VI show the results of the electrical performance measurements, where it can be seen that the electrical output is 280 W in both cases. The open-circuit voltage for the parallel-connected MCT was 197 V, and for the series-connected MCT, the open-circuit voltage was 394 V, with short-circuit currents of 2.3 and 1.2 A, respectively.

Table III. MCT system measurements for both receiver interconnections.

Receivers interconnection	Series	Parallel
Number of sub-modules	20	20
Number of cells per sub-module	30	30
Number of cells in series (Ns)	600	300
Number of cells in parallel (Np)	NIL	2 X 300
Number of cells	600	600
Approximate Isc at 1 sun and Tcell 25 °C [A]	0.109	0.218
Approximate Voc at 1 sun and Tcell 25 °C [V]	398	199

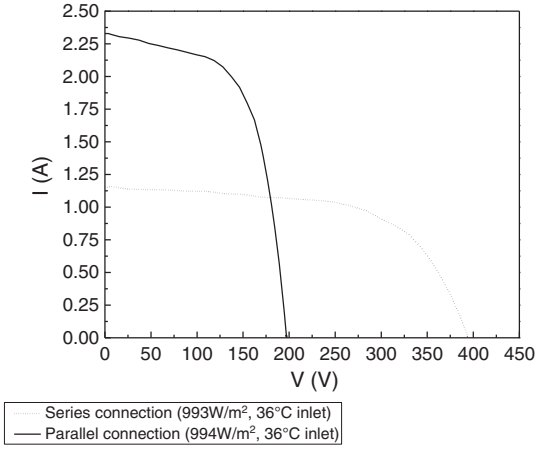

Figure 7. *I–V* curves for series and parallel receiver interconnections from the MCT instantaneous electrical performance measurements reported in Table VI.

Table IV. Meteorological data for the MCT instantaneous measurements taken at noon on 25th August 2011.

Parameter	Series	Parallel
Normal direct irradiance (W/m^2)	997	997
Ambient temperature (°C)	18	18
Global irradiance in the plane of incidence (W/m^2)	1045	1049
Effective direct irradiance (cosine corrected) (W/m^2)	995	994
Effective direct irradiance (cosine corrected) on the box (W)	3582	3578

Table V. Thermal output data corresponding to the instantaneous *I–V* curves taken on the 25 August 2011 [(12:09:39 and 12:06:35]) for the two MCT configurations.

Parameter	Series	Parallel
Flow rate (kg/s)	0.092	0.093
Inlet temperature, T_{inlet} (°C)	36	36
Outlet temperature, T_{outlet} (°C)	42	42
Thermal output power (W_{th})	2320	2540
Thermal efficiency (%)	65%	71%

Table VI. Electrical output data corresponding to the instantaneous *I–V* curves taken on 25 August 2011 (12:09:39 and 12:06:35) for the two MCT configurations.

Parameter	Series	Parallel
Open-circuit voltage, V_{OC} (V)	394	197
Short-circuit current, I_{sc} (A)	1.15	2.33
Maximum power point, MPP (W)	276	280
Current at maximum power point, I_{MPP} (A)	0.97	1.92
Voltage at maximum power point, V_{MPP} (V)	284	146
System efficiency, Eff (%)	8%	8%
Fill factor, FF (%)	61%	61%

Considering that the nominal short-circuit current at 1 sun is 0.109 A for the series interconnection, and of 0.218 A for the parallel interconnection, it can be deduced that the MCT system is working at an optical concentration ratio of approximately 10.6 suns. This value is well below the 20X geometric concentration ratio (Table II), so a careful analysis of losses in the system must be conducted, including optical efficiencies, shading effects, optical and electrical mismatch, soiling and so on. One factor that influenced optical losses in this prototype MCT was mirror reflectivity degradation caused by extended outdoor exposure while the box was unsealed to allow experimental access. The thermal output is approximately 2400 Wth for both serial and parallel interconnection. As expected, the change in interconnection configuration does not significantly affect the total system output.

It is important to note that, depending on the angle of incidence of the sun, and the orientation of the tracking system, the individual receivers within an MCT unit might be illuminated non-uniformly (for example, during early morning and late afternoon), and therefore, have different electrical performance. In this specific case, the parallel interconnection would have advantages over series interconnection. Another issue requiring consideration is that, depending on the pre-determined temperature difference between inlet and outlet, the average temperature of the cells of the second series-connected receiver could be significantly higher than the first receiver, with a consequent reduction in electrical output. Finally, issues such as the series–parallel interconnections of MCT units in a complete installation must be analysed in terms of the interconnection topology and electrical and thermal optimisation of the system.

4.2. Full-day performance

The hybrid MCT was operated over the span of a full day, with thermal and electrical performance logged as a function of time. The tilt angle of the system was fixed during the day at 35°. During the days when tests were conducted, from May 2011 to August 2011, the weather was clear, cold and sunny, with light winds: typical of good winter weather in Canberra. The results presented here were obtained for the combined electrical and thermal performance of the first MCT hybrid PV-T prototype unit.

Two modes of cooling were monitored during the initial testing regime: *open-loop mode*, in which the cooling water flowed directly from the tap (i.e. constant temperature); and *closed-loop mode*, in which the water was recirculated through a closed circuit and stored in a water tank as explained in the previous section. Whereas the open-loop mode allowed us to characterise the system easily at a constant inlet temperature, the closed-loop mode provided a configuration similar to real operating conditions. In this latter mode, the temperature of the water in the tank increases until the water temperature reaches a pre-set maximum value, at which point an over-heating control system is triggered in order to protect the photovoltaic receivers from damage at high temperatures.

Figure 8 shows the thermal performance of the system during one of the open-loop testing days (23 June 2011),

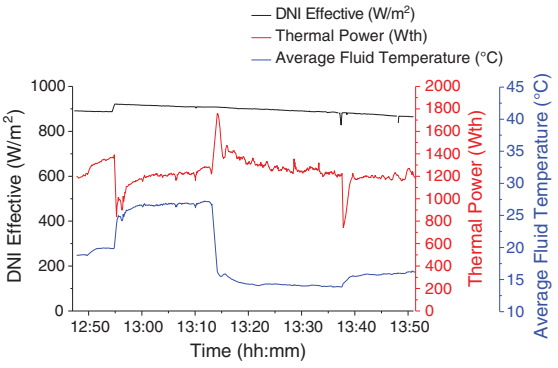

Figure 8. Thermal performance of the system operating in open-loop mode over a period after noon on 23 June 2011. The incident direct irradiance and the average fluid temperature (inlet temperature and outlet temperature) are also presented.

with constant inlet supply temperature and output as a function of variations on the flow rate of the tap water. Figure 9 depicts the corresponding inlet and outlet temperatures, ambient temperature and flow rate. The output variations arising from changes in the flow rate, which affect the outlet temperature and total thermal output, can be clearly seen. In particular, the spikes in thermal power evident in Figure 8 are a direct result of variations in the flow rate and illustrate a latency, or thermal 'capacitive effect', which is a characteristic of the volume of thermal transfer fluid within the MCT system, along with the thermal mass of the receiver system. In fact, under constant DNI operating conditions, the thermal mass of the receiver system can be calculated from the change in flow rate, the change in output temperature, and the time taken for the system to reach equilibrium output power.

After a series of tests operating the system in open-loop, the cooling circuit was changed to a closed-loop configuration, which included a small storage tank, as explained in Section 3. Figure 10 shows the total performance of the MCT system during one of the testing days (25 August 2011), including the electrical power output and the thermal power output. Incident direct irradiance and mean fluid temperature are also depicted. From these results, it can be seen how the electrical output drops as the fluid temperature rises. For this series of tests, the thermal transfer fluid flow rate was controlled so that the fluid temperature did not exceed 60 °C. Therefore, at two different moments, the thermal transfer fluid temperature was cooled down to approximately 30 °C, as can be observed in the temperature profile, with two well-defined peaks. These two changes in temperature affect both the electrical and thermal output. The electrical output increases as temperature drops, owing to the increase in cell voltage, and the thermal output also increases with the drop in temperature, owing to reduced thermal losses arising from a smaller temperature difference between the receiver operating temperature and ambient conditions. The spikes in thermal output — or 'apparent' thermal output — arise from the same circumstances described for the Figure 8 data. In real

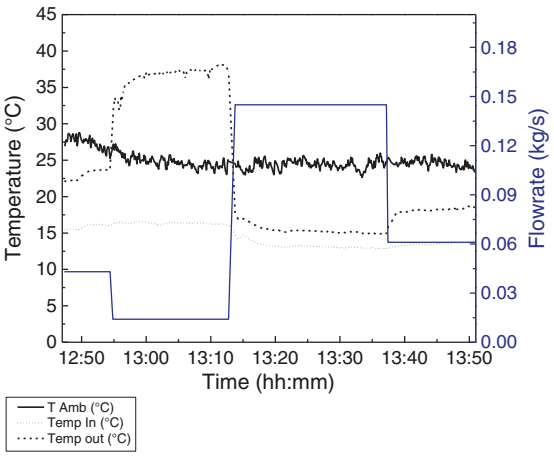

Figure 9. Inlet and outlet fluid temperature dependence on [1]thermal transfer fluid flow rate, with ambient temperature for reference over the test period (23 June 2011).

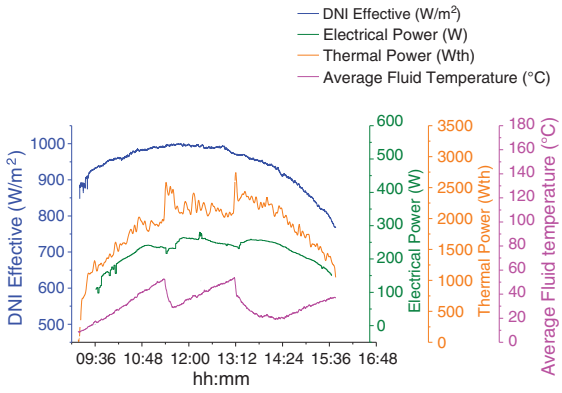

Figure 10. Electrical and thermal performance over the span of 25 August 2011. Incident direct irradiance and average fluid temperature are also depicted.

operating conditions in commercial systems, a compromise between the combined electrical and thermal output of the system will be determined, so the system functions optimally according to the consumer value and demand of electricity and hot water. Inlet and outlet fluid temperatures are depicted in Figure 11, where two main peaks, corresponding to the points at which the control system changed operation mode to cool down the receiver so the fluid temperature did not exceed 60 °C, can be observed.

4.3. Operating concentration ratio

The effective concentration ratio in the system can be calculated by observing the short-circuit current, to arrive at a value of about 10X (Figure 12), which is roughly half the 20X geometric concentration ratio described in Section 2. In order to understand the low effective concentration, an analysis of the total losses in the system must be

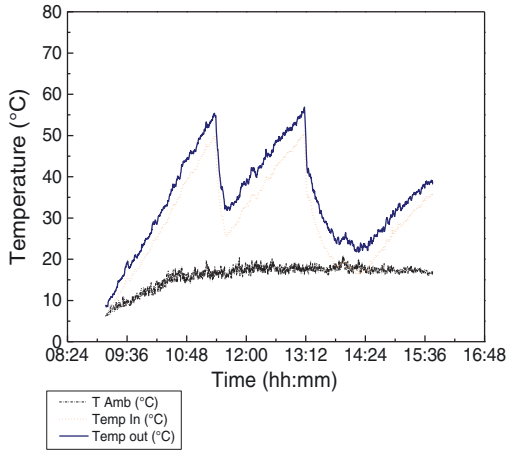

Figure 11. Ambient temperature, inlet fluid temperature and outlet fluid temperature over the span of a day (25 August 2011). Inlet and outlet temperatures show two main peaks corresponding to the control system altering temperatures for the receiver so as not to exceed 60°C.

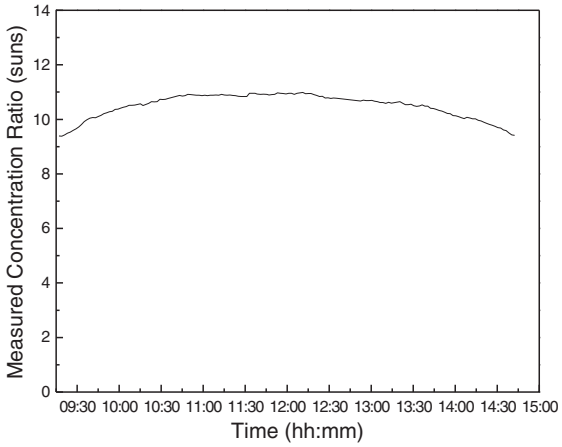

Figure 12. Measured concentration ratio in the MCT unit during 27 July 2011.

carefully conducted. As already mentioned, one factor that has influenced optical losses in this initial prototype is the degradation of the mirrors that reduced their reflectivity caused by extended exposure outdoors with an inadequate box seal. As previously mentioned, optical losses in this prototype MCT were uncharacteristically high owing to mirror reflectivity degradation caused by extended outdoor exposure while the box was unsealed to allow ease of experimental access. An improved experimental procedure has been devised to allow experimental access while maintaining seal protection.

4.4. Voc temperature coefficient

Figure 13 shows the value of the open-circuit voltage, Voc, as a function of the average fluid temperature in the receivers. The calculated temperature coefficient of the system as a function of the average fluid temperature is -0.541 V/°C at around 10X. This MCT unit temperature coefficient can be reduced to the temperature coefficient of the individual cells:

$$-0.541\ \text{V}/^\circ\text{C}/300\ \text{cells in series (receiver parallel connection)} = \mathbf{-1.8\ mV}/^\circ\mathbf{C}$$

The temperature coefficient of Voc of the same cells measured in a Flash I-V system indoors was $\mathbf{-1.8\,mV/^\circ C}$. This confirms that the result is consistent with the measured behaviour of individual cells.

4.5. Electrical efficiency temperature coefficient

Figure 14 shows the electrical efficiency as a function of the average fluid temperature during a testing day, 27 July 2011. The calculated value of the electrical efficiency temperature coefficient is $\mathbf{-0.27\%/^\circ C}$ at the operating optical concentration ratio of 10X.

4.6. Thermal efficiency

The thermal performance of the prototype MCT has also been analysed, with the thermal efficiency presented as a function of the value of T_{in}-T_{amb}/G (Figure 15), where G is the effective irradiance on the MCT unit. The scatter in the data is primarily caused by the high measurement uncertainty arising from a combination of low-resolution thermocouples and small temperature differences encountered in this initial test. High-resolution thermocouples, used in later experiments, reduced this uncertainty.

4.7. Summary

The initial results from the electrical and thermal performance measurements of the ANU-Chromasun MCT prototype installed at ANU have been presented, including the results from instantaneous and full-day monitoring. These measurements show that the combined efficiency of the

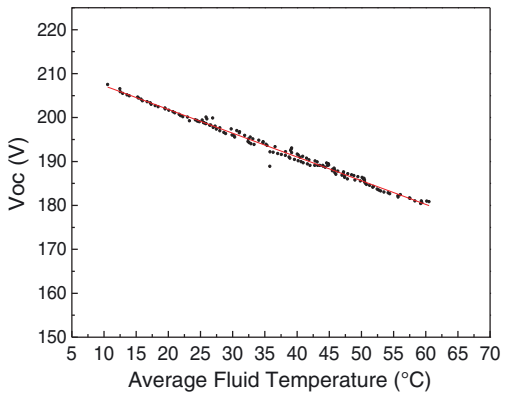

Figure 13. Voc of the complete MCT system, for receivers in parallel interconnection format, as a function of the average fluid temperature circulating through the receivers (27 July 2011).

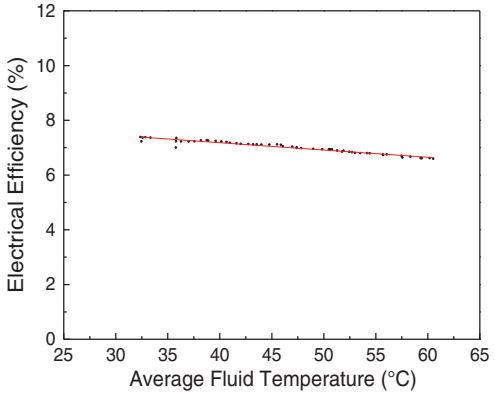

Figure 14. Electrical efficiency of the complete MCT system as a function of the average thermal transfer fluid temperature in the MCT unit on 27 July 2011.

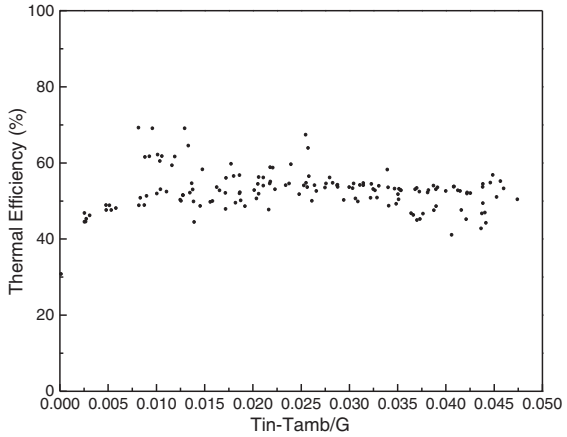

Figure 15. Thermal efficiency as a function of Tin-Tamb/G over the span of 27 July 2011.

prototype MCT hybrid PV-T system can achieve 70% instantaneously and 60% over the span of a full day.

System performance aspects that need to be considered in the future include the effect of the different interconnection configuration of the receivers within the box on the total system output. In general, the receivers will not be evenly illuminated over the entire day owing to the nature of the linear Fresnel collector, so the optimum electrical configuration must be explored in detail.

With respect to the consideration of real operating conditions using commercial systems, the interaction between the electrical and thermal output of the system must be thoroughly understood in terms of combined system performance, in order to determine an optimum operating point according to the consumer value and demand of electricity and hot water.

5. POWER LOSSES IN THE MICRO-CONCENTRATOR SYSTEM

Losses in the MCT system can be grouped into four broad categories: inability to efficiently use direct beam radiation; system optical losses; losses associated with the photovoltaic aspects of the receivers; and thermal losses, which also include the specific considerations for hybrid systems, such as the reduced energy available for the thermal component because a proportion of the incident energy on the receiver, determined by the solar cell efficiency, is extracted by the solar cells. The origins of the power losses are described briefly next, and a preliminary estimation of the electrical and thermal output is presented according to the losses study. This is an important and complex area to be considered only briefly in this paper; it will be the substance of a comprehensive subsequent paper.

The very first power loss in the concentrator system is reduced sunlight collection, because a concentrating collector can only utilise direct-beam radiation, which is typically 70–90% of the global radiation at a good site, along with some circumsolar radiation and a small fraction of diffuse radiation depending on the acceptance angle of the concentration system.

5.1. Optical losses

Optical losses encompass the characteristics of the optical system and its performance; from the materials themselves, to the limitations of the geometric design, to the total system operation under tracking. These can be itemised as follows:

- Optical efficiency of the primary optics: The glass cover transmittance has been measured at *95%*, (recently been improved with the use of AR-coated glass), and the Alanod MIRO® SILVER mirrors have a reflectivity of *95%* [9]. However, if the system sealing is inadequate, water moisture entering into the enclosure can rapidly degrade the reflectivity of the mirrors.
- Optical limitations: The MCT uses linear Fresnel mirrors, which typically collect up to *70%* of the light of an equivalent parabolic mirror, [10,11].
- Mirror discontinuities: The MCT eliminates longitudinal gaps between the mirrors, reducing shadows on the receivers and a consequent loss of power, but do have gaps in the orthogonal direction owing to the Fresnel nature of optic array.
- Optical efficiency of secondary optics: The MCT secondary optics consists of reflective winglets, made of the same material as the primary mirrors.
- Dispersion and scattering: Local defects in the optical surfaces and soiling of the surfaces cause scattering of the incident light, with some fraction missing the focal region. The MCT, with mirrors located inside and protected from dirt and dust, minimise mirror scattering, with the major soiling corresponding to the cover glass. This approach ensures that the losses caused by soiling are similar to the losses in a flat PV panel, about *4–8%*, which is much less significant than with a parabolic mirror, which has scattering losses up to 25% [12,13].
- Sealing of the system: This is a critical issue not only for protecting the cells and accommodating different thermal expansions of volume of air inside but also because of condensation of trapped water vapour, which can seriously degrade concentrating optical performance.
- Alignment of optics and system tracking. Correct alignment between the optics and the receivers is critical in concentrating systems [14], and tracking errors must be minimised in order to reduce power loss.

5.2. Photovoltaic losses

Photovoltaic losses include all performance issues related to the solar cell and its packaging into a final module:

- Module efficiency is limited by the initial cell efficiency, and hence the receiver efficiency once the cells have been encapsulated. Losses include:

- Optical efficiency of the receiver, determined primarily by material absorption losses and Fresnel reflection.
- Cell mismatch. The CPV receiver series-connected string is limited by the performance of the worst cell in the string. Cell mismatch, and non-uniform longitudinal flux distribution, can seriously degrade system performance.
- Cell packing. Owing to functional constraints, gaps exist between cells, thus limiting the utilisation of incoming light.
- Ohmic losses. Interconnecting resistance in the circuit path and busbars of the cells [15].
- Temperature losses. Under high cell operating temperatures, the cell voltage decreases, with a commensurate loss in efficiency. In general, for silicon solar cells, the efficiency loss with temperature is about −0.4%/°C.
- Influence of end-effects can be significant for concentrators tracking in only one axis with light at low angles in the longitudinal direction.

5.3. Thermal losses

Thermal losses include radiative losses, convective losses, and thermal transfer losses. These losses have been quantified by Joe Coventry by experimentation with the previous CHAPS receivers [16]. However, for hybrid CPV-T receivers, a fraction of the incident light, corresponding to the efficiency of the solar cells, is no longer available for thermal conversion.

5.4. Estimated electrical and thermal output according to the power loss analysis

A non-optimistic total loss analysis summary for the MCT system according to tests performed on the different components, along with theoretical estimations conducted for sources of some of the other losses, is shown in Table VII. Most of the losses are associated with the optical system. It can be seen that the overall electrical efficiency is about 8% and the thermal efficiency is 41%, achieving a combined efficiency of 49%. With reasonable optimisation of the optical system, the electrical efficiency could achieve 12% and the thermal efficiency 54%, with a combined efficiency of 66%, as shown in Table VIII. Therefore, a comprehensive analysis of all the power losses in the system is necessary. The analysis will allow thorough system optimisation, taking into account the improvement in performance and the associated costs to achieve that improvement.

Table VII. Electrical and thermal estimated efficiencies of the MCT system based on a preliminary power loss analysis for a non-optimistic scenario with non-optimised optics.

Reduced efficiency of the MCT owing to...	PV (%)	Thermal (%)
Reduced use of solar radiation		
Direct beam only	85	85
Optical losses		
Optical efficiency of primary optics		
Glass transmittance	95	95
Mirror reflectivity	92	92
Optical limitations		
Linear Fresnel mirrors + mirror shadowing	85	85
Optical efficiency of secondary optics (winglets)	98	98
Dispersion optical efficiencies	90	90
Photovoltaic losses		
Module efficiency		
Optical efficiency of receiver (encapsulation)	96	—
Solar cell efficiency	18	—
Cell mismatch	98	—
Cell packing + ohmic losses	95	—
Temperature losses at 65 °C	96	—
Interconnection losses (series or parallel)	97	—
Thermal losses		
Radiative losses	—	98
Convective losses	—	95
Thermal transfer losses	—	98
Reduced light for thermal in a hybrid PV-T receiver	—	80
Overall system efficiency	8	41

6. CONCLUSION

First results of the electrical and thermal performance of the ANU-Chromasun MCT prototype installed at ANU facilities have been presented, including results from instantaneous and full-day monitoring, which show that the combined efficiency of the system can exceed 70%. Instantaneous performance included two possible receiver interconnection configurations within the system: series and parallel.

Initial results were obtained for an effective direct irradiance incident onto the system of 994 W/m^2, with both receivers evenly illuminated, an inlet fluid temperature of 36 °C and an outlet temperature 42 °C. Under these conditions, the electrical output was approximately 280 W in both cases, with a corresponding thermal output of around 2400 Wth. As expected, under even and uniform illumination conditions for both receivers, the different interconnection configuration did not affect the total system output. However, as the receivers will not be evenly illuminated over the entire day, the optimum electrical configuration must be explored.

The hybrid MCT was also operated over the span of a full day. For this series of tests, the thermal transfer fluid flow rate was controlled so that it did not exceed 60 °C. Therefore, at different periods during the day, the thermal fluid temperature was cooled to approximately 30 °C, causing an increase in the electrical output of the system but with a lower outlet temperature. In real operating conditions in commercial systems, a compromise between the combined electrical and thermal outputs of the system must be met, so that the system operates at an optimum point according to the consumer value and demand of

Table VIII. Electrical and thermal estimated efficiencies of the MCT system based on a preliminary power loss analysis for an optimised system based solely on optics improvement.

Reduced efficiency of the MCT owing to...	PV (%)	Thermal (%)
Reduced use of solar radiation		
Direct beam only	85	85
Optical losses		
Optical efficiency of primary optics		
Glass transmittance	96	96
Mirror reflectivity	95	95
Optical limitations		
Linear Fresnel mirrors + mirror shadowing	97	97
Optical efficiency secondary optics (winglets)	98	98
Dispersion optical efficiencies	98	98
Photovoltaic losses		
Module efficiency		
Optical efficiency of receiver (encapsulation)	96	—
Solar cell efficiency	20	—
Cell mismatch	98	—
Cell packing + ohmic losses	95	—
Temperature losses at 65 °C	96	—
Interconnection losses (series or parallel)	97	—
Thermal losses		
Radiative losses	—	98
Convective losses	—	98
Thermal transfer losses	—	98
Reduced light for thermal in a hybrid PV-T receiver	—	80
Overall system efficiency	12	54

electricity and hot water. The temperature coefficients of the PV system with respect to the average fluid temperature were also calculated: the V_{oc} temperature coefficient of -1.8 mV/°C and an electrical efficiency temperature coefficient of -0.27 %/°C at the operating concentration of 10X. Over the span of a day, the average electrical efficiency was 8%, and the average thermal efficiency was 50%.

Finally, a preliminary analysis of the power losses of the system has also been reported for two different scenarios, which show the importance of such analysis for future system optimisations. The analysis should consider not only efficiency improvements but also the associated cost required to achieve those improvements.

ACKNOWLEDGEMENTS

This work has been supported by the Department of Resources, Energy and Tourism, Australia, in the framework of the Asia-Pacific Partnership on Clean Development and Climate through the funding of the project 'Increasing Efficiency of Linear Concentrators to Capture Solar Energy' (RDG-06-23).

REFERENCES

1. Smeltink J, Blakers A, Hiron S. The ANU 20 kW PV/Trough concentrator. 16th European Photovoltaic Solar Energy Conference, 2000, Glasgow, UK.
2. Smeltink J, Blakers A, Coventry J. A 40 kW roof mounted PV thermal concentrator system. 22nd European Photovoltaic Solar Energy Conference and Exhibition, 2007, Milan, Italy.
3. Walter D, Everett V, Blakers A, Vivar M, Harvey J, Muric-Nesic J, Ratcliff T, Surve S, Van Scheppingen R, Le Lievre P, Greaves M, Tanner A. A 20-sun hybrid PV-thermal linear micro-concentrator system for urban rooftop applications. 35th IEEE Photovoltaic Specialists Conference, 2010; Honolulu, HI; 831–836.
4. Everett V, Harvey J, Vivar M, Thomsen E, Fuentes M, Ebert M, Le Lievre P, Greaves M, Tanner A, Blakers A. A linear Fresnel Hybrid PV/thermal micro-concentrator system for rooftop integration. 25th European Photovoltaic Solar Energy Conference and Exhibition (25th EU PVSEC)/5th World Conference on Photovoltaic Energy Conversion (WCPEC-5), 2010, Valencia, Spain; 3937–3941.
5. Everett V, Walter D, Harvey J, Vivar M, Van Scheppingen R, Surve S, Blakers A. Enhanced longitudinal and lateral flux uniformity for linear Fresnel reflectors in concentrating photovoltaic systems. 25th European Photovoltaic Solar Energy Conference and Exhibition (25th EU PVSEC)/5th World Conference on Photovoltaic Energy Conversion (WCPEC-5), Valencia (Spain), September 2010; 1060–1062.
6. Walter D, Everett V, Vivar M, Harvey J, Van Scheppingen R, Surve S, Muric-Nesic J, Blakers A. A monolithic micro-concentrator receiver for a hybrid PV-thermal system: preliminary performance. 6th International Conference on Concentrating Photovoltaic, AIP Conference Proceedings Volume 1277, 2010; 70–73.
7. Vivar M, Everett V, Blakers A, Walter D, Harvey J, Van Scheppingen R, Surve S, Muric-Nesic J. Designing CPV receivers with reliability: early evaluation of components. 6th International Conference on Concentrating Photovoltaic, AIP Conference Proceedings 1277, 2010; 233–236.
8. Everett V, Walter D, Harvey J, Vivar M, Van Scheppingen R, Surve S, Blakers A. A closed loop tracking system for a linear Fresnel hybrid PV/thermal micro-concentrator system. 25th European Photovoltaic Solar Energy Conference and Exhibition (25th EU PVSEC)/5th World Conference on Photovoltaic Energy Conversion (WCPEC-5), Valencia (Spain), September 2010; 1063–1065.
9. ALANOD MIRO® SILVEr, Alanod 4270 Technical Datasheet, http://www.alanod.com [accessed on 5 March 2012]

10. Häberle A, Zahler C, Lerchenmüller H, Mertins M, Wittwer C, Trieb F, Dersch J. The Solarmundo line focussing Fresnel collector. Optical and thermal performance and cost calculations. SolarPaces Conference, Zürich, Switzerland, 2002.
11. El Gharbi N, Derbal H, Bouaichaoui S, Said N. A comparative study between parabolic trough collector and linear Fresnel reflector technologies. *Energy Procedia* 2011; **6**: 565–572.
12. Vivar M, Antón I, Pachón D, Sala G. Third-generation EUCLIDES concentrator results. *Progress in Photovoltaics: Research and Applications* 2011. DOI: 10.1002/pip.1136, in press.
13. Vivar M, Herrero R, Antón I, Martínez-Moreno F, Moretón R, Sala G, Blakers A, Smeltink J. Effect of soiling in CPV systems. *Solar Energy* 2010; **84**: 1327–1335.
14. Antón I, Sala G. Losses caused by dispersion of optical parameters and misalignments in PV concentrators. *Progress in Photovoltaics: Research and Applications* 2005; **13**(4): 341–352.
15. Mallick T, Eames P, Norton B. Power losses in an asymmetric compound parabolic photovoltaic concentrator. *Solar Energy Materials and Solar Cells* 2007; **91**: 1137–1146.
16. Coventry J. A solar concentrating photovoltaic/thermal collector, Ph.D. Thesis, The Australian National University, 2004.